Research Article | Vol. 24, No. 18 | 5 Sep 2016 | OPTICS EXPRESS 21038

Optics EXPRESS

1.3-μm InAs quantum-dot micro-disk lasers on V-groove patterned and unpatterned (001) silicon

QIANG LI,[1,5] YATING WAN,[1,5] ALAN Y. LIU,[2,5] ARTHUR C. GOSSARD,[2,3] JOHN E. BOWERS,[2,3] EVELYN L. HU,[4] AND KEI MAY LAU[1,*]

[1]*Department of Electronic and Computer Engineering, Hong Kong University of Science and Technology, Clear Water Bay, Kowloon, Hong Kong*
[2]*Materials Department, University of California Santa Barbara, Santa Barbara, California 93106, USA*
[3]*Department of Electrical and Computer Engineering, University of California Santa Barbara, Santa Barbara, California 93106, USA*
[4]*School of Engineering and Applied Sciences, Harvard University, Cambridge, MA 02138, USA*
[5]*Q. Li, Y. Wan and A. Y. Liu contributed equally to this work*
[*]*eekmlau@ust.hk*

Abstract: We report comparison of lasing dynamics in InAs quantum dot (QD) micro-disk lasers (MDLs) monolithically grown on V-groove patterned and planar Si (001) substrates. TEM characterizations reveal abrupt interfaces and reduced threading dislocations in the QD active regions when using the GaAs-on-V-grooved-Si template. The improved crystalline quality translates into lower threshold power in the optically pumped continuous-wave MDLs. Concurrent evaluations were also made with devices fabricated simultaneously on lattice-matched GaAs substrates. Lasing behaviors from 10 K up to room temperature have been studied systematically. The analyses spotlight insights into the optimal epitaxial scheme to achieve low-threshold lasing in telecommunication wavelengths on exact Si (001) substrates.

OCIS codes: (140.5960) Semiconductor lasers; (140.3948) Microcavity devices; (230.5590) Quantum-well, -wire and -dot devices.

References and links

1. D. Liang and J. E. Bowers, "Recent progress in lasers on silicon," Nat. Photonics **4**(8), 511–517 (2010).
2. H. Rong, R. Jones, A. Liu, O. Cohen, D. Hak, A. Fang, and M. Paniccia, "A continuous-wave Raman silicon laser," Nature **433**(7027), 725–728 (2005).
3. S. Wirths, R. Geiger, N. von den Driesch, G. Mussler, T. Stoica, S. Mantl, Z. Ikonic, M. Luysberg, S. Chiussi, J. M. Hartmann, H. Sigg, J. Faist, D. Buca, and D. Grützmacher, "Lasing in direct-bandgap GeSn alloy grown on Si," Nat. Photonics **9**(2), 88–92 (2015).
4. J. E. Bowers, J. T. Bovington, A. Y. Liu, and A. C. Gossard, "A path to 300 mm hybrid silicon photonic integrated circuits," in *Optical Fiber Communication Conference* (2014), pp 1-3.
5. Z. Zhou, B. Yin, and J. Michel, "On-chip light sources for silicon photonics," Light Sci. Appl. **4**(11), e358 (2015).
6. J. Yang, P. Bhattacharya, and Z. Mi, "High-performance $In_{0.5}Ga_{0.5}As$/GaAs quantum-dot lasers on silicon with multiple-layer quantum-dot dislocation filters," IEEE Trans. Electron Dev. **54**(11), 2849–2855 (2007).
7. A. Lee, Q. Jiang, M. Tang, A. Seeds, and H. Liu, "Continuous-wave InAs/GaAs quantum-dot laser diodes monolithically grown on Si substrate with low threshold current densities," Opt. Express **20**(20), 22181–22187 (2012).
8. M. Tang, S. Chen, J. Wu, Q. Jiang, V. G. Dorogan, M. Benamara, Y. I. Mazur, G. J. Salamo, A. Seeds, and H. Liu, "1.3-μm InAs/GaAs quantum-dot lasers monolithically grown on Si substrates using InAlAs/GaAs dislocation filter layers," Opt. Express **22**(10), 11528–11535 (2014).
9. A. Y. Liu, C. Zhang, J. Norman, A. Snyder, D. Lubyshev, J. M. Fastenau, A. W. K. Liu, A. C. Gossard, and J. E. Bowers, "High performance continuous wave 1.3 μm quantum dot lasers on silicon," Appl. Phys. Lett. **104**(4), 041104 (2014).
10. A. Y. Liu, R. W. Herrick, O. Ueda, P. M. Petroff, A. C. Gossard, and J. E. Bowers, "Reliability of InAs/GaAs quantum dot lasers epitaxially grown on silicon," IEEE J. Sel. Top. Quantum Electron. **21**(6), 1900708 (2015).
11. A. Y. Liu, S. Srinivasan, J. Norman, A. C. Gossard, and J. E. Bowers, "Quantum dot lasers for silicon photonics," Photonics Res. **3**(5), B1–B9 (2015).

#272375 http://dx.doi.org/10.1364/OE.24.021038
Journal © 2016 Received 26 Jul 2016; revised 18 Aug 2016; accepted 21 Aug 2016; published 31 Aug 2016

Optics EXPRESS

12. S. Chen, W. Li, J. Wu, Q. Jiang, M. Tang, S. Shutts, S. N. Elliott, A. Sobiesierski, A. J. Seeds, I. Ross, P. M. Smowton, and H. Liu, "Electrically pumped continuous-wave III–V quantum dot lasers on silicon," Nat. Photonics **10**(5), 307–311 (2016).
13. Y. Wan, Q. Li, Y. Geng, B. Shi, and K. M. Lau, "InAs/GaAs quantum dots on GaAs-on-V-grooved-Si substrate with high optical quality in the 1.3 μm band," Appl. Phys. Lett. **107**(8), 081106 (2015).
14. Q. Li, K. W. Ng, and K. M. Lau, "Growing antiphase-domain-free GaAs thin films out of highly ordered planar nanowire arrays on exact (001) silicon," Appl. Phys. Lett. **106**(7), 072105 (2015).
15. Y. Wan, Q. Li, A. Y. Liu, A. C. Gossard, J. E. Bowers, E. L. Hu, and K. M. Lau, "Optically pumped 1.3 μm room-temperature InAs quantum-dot micro-disk lasers directly grown on (001) silicon," Opt. Lett. **41**(7), 1664–1667 (2016).
16. Y. Wan, Q. Li, A. Y. Liu, W. W. Chow, A. C. Gossard, J. E. Bowers, E. Hu, and K. M. Lau, "Sub-wavelength InAs quantum dot micro-disk lasers epitaxially grown on exact Si (001) substrates," Appl. Phys. Lett. **108**(22), 221101 (2016).
17. Y. Wan, Q. Li, A. Y. Liu, A. C. Gossard, J. E. Bowers, E. L. Hu, and K. M. Lau, "Temperature characteristics of epitaxially grown InAs quantum dot micro-disk lasers on silicon for on-chip light sources," Appl. Phys. Lett. **109**(1), 011104 (2016).
18. Q. Li, C. W. Tang, and K. M. Lau, "Growth of ultra-high mobility $In_{0.52}Al_{0.48}As/In_xGa_{1-x}As$ ($x \geq 53\%$) quantum wells on Si substrates using InP/GaAs buffers by metalorganic chemical vapor deposition," Appl. Phys. Express **7**(4), 045502 (2014).
19. Y. Bogumilowicz, J. M. Hartmann, R. Cipro, R. Alcotte, M. Martin, F. Bassani, J. Moeyaert, T. Baron, J. B. Pin, X. Bao, Z. Ye, and E. Sanchez, "Anti-phase boundaries–Free GaAs epilayers on "quasi-nominal" Ge-buffered silicon substrates," Appl. Phys. Lett. **107**(21), 212105 (2015).
20. Q. Li, X. Zhou, C. W. Tang, and K. M. Lau, "Material and device characteristics of metamorphic $In_{0.53}Ga_{0.47}As$ MOSHEMTs grown on GaAs and Si substrates by MOCVD," IEEE Trans. Electron Dev. **60**(12), 4112–4118 (2013).
21. R. Alcotte, M. Martin, J. Moeyaert, R. Cipro, S. David, F. Bassani, F. Ducroquet, Y. Bogumilowicz, E. Sanchez, Z. Ye, X. Y. Bao, J. B. Pin, and T. Baron, "Epitaxial growth of antiphase boundary free GaAs layer on 300 mm Si(001) substrate by metalorganic chemical vapour deposition with high mobility," APL Mater. **4**(4), 046101 (2016).
22. A. Y. Liu, C. Zhang, A. Snyder, D. Lubyshev, J. M. Fastenau, A. W. K. Liu, A. C. Gossard, and J. E. Bowers, "MBE growth of P-doped 1.3 μm InAs quantum dot lasers on silicon," J. Vac. Sci. Technol. B **32**(2), 02C108 (2014).

1. Introduction

Fusing photonic circuits with the advanced silicon technology can break the cost barrier of optoelectronics, essential to enabling the transition from copper to optical interconnects in future data centers [1]. In this regard, an on-chip light source represents a vital component, but has been a major obstacle hindering the development of silicon photonics. Although attempts have been made to overcome the indirect bandgap limitation in Si and group-IV compatible alloys, a highly efficient silicon-based laser that is on par with state-of-the-art III-V lasers remains elusive [2, 3]. Integration of III-V laser diodes on silicon is arguably the most viable path to leverage the economies of scale of silicon while maintaining the highest efficiency and yield [4, 5]. Over the last few decades, various approaches to achieve III-V photonics on silicon have been pursued, including flip-chip integration, bonding technology, and heteroepitaxial growth. Despite the fact that direct epitaxy of III-V lasers on silicon is a truly monolithic approach desirable in the long term, this technology has lagged far behind [1] because of the fundamental challenges in mitigating issues brought by the lattice mismatch and thermal mismatch between III-V materials and silicon. The high sensitivity of semiconductor lasers to crystalline defects generated in heteroepitaxy makes the task formidable. Recent advances in growing high performance InAs quantum dot (QD) lasers on Si substrates revealed the great potential of utilizing dense and spatially isolated quantum dots to circumvent crystal defects in heteroepitaxy, marking a big step towards potential commercial success of integrated silicon photonics [6–12]. To eliminate antiphase-domains (APDs), all the work reported so far, however, strongly relies on the use of offcut Si substrates. Previously, we have introduced GaAs on V-groove patterned silicon (GoVS) templates using CMOS-compatible, exact (001) silicon wafers without offcut [13, 14] and demonstrated 1.3-μm InAs QD micro-disk lasers (MDLs) [15–17]. Compared to the use of planar Si substrates, growing quantum-dot lasers on V-groove patterned Si substrates may

Optics EXPRESS

benefit from the reduced threading dislocations and buffer thickness. It is therefore of great importance to establish correlations between the buffer material quality and device characteristics. In this paper, we have grown and fabricated 1.3-μm InAs quantum-dot micro-disk lasers on both V-groove patterned and unpatterned (001) Si substrates. A systematic study of the defect properties and lasing dynamics of the micro-disk lasers was carried out. Benchmarking of the QD lasers on the two types of GaAs-on-(001) Si templates against devices fabricated on lattice-matched GaAs substrate was also conducted. The overall assessment links superior device characteristics with improved crystalline quality of the epitaxial template structures on silicon.

2. Experiments and results

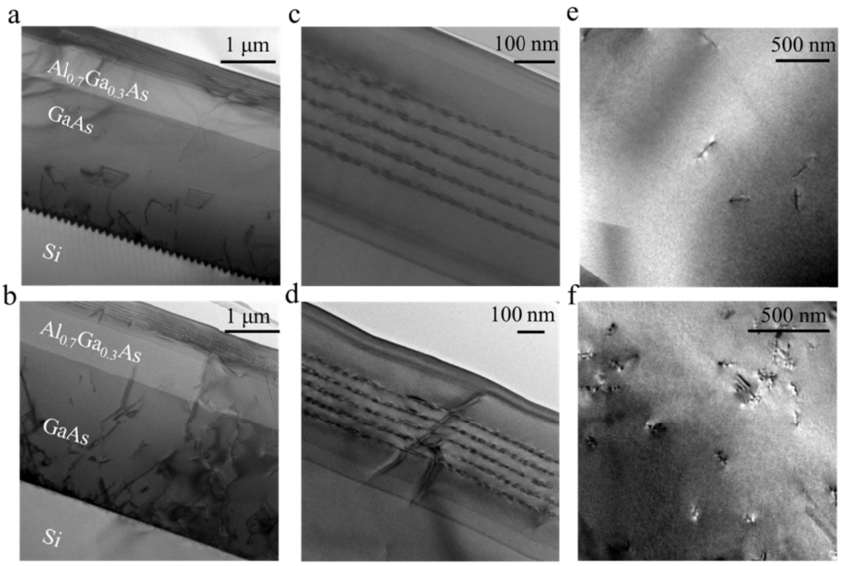

Fig. 1. Cross-sectional TEM image of the MDLs grown on (a) the GoVS template and (b) the planar Si template; Cross-sectional TEM image of the five-layer stack InAs DWELL on (c) the GoVS template and (d) the planar Si template; Plan-view TEM images showing the threading dislocations in active regions on (e) the GoVS template and (f) the planar Si template.

We first prepared two GaAs-on-(001) Si templates by metalorganic chemical vapor deposition (MOCVD), one on a V-groove patterned Si substrate and the other on a planar Si substrate. The V-groove pattern, aligned in the [110] direction with a pitch of 130 nm, was created by a SiO_2 stripe-masked Si wafer using anisotropic silicon wet etching in a 45% KOH solution. MOCVD selective area growth was performed to generate an array of GaAs planar nanowires inside the V-grooves. Subsequent removal of the SiO_2 mask and coalesced growth of the GaAs nanowires led to the 1 μm GaAs-on-V-grooved-silicon template [14]. For the growth on planar Si, a two-step method has been employed. Specifically, a thin (~10 nm) GaAs nucleation layer was deposited at a temperature around 400 °C, followed by the growth of a 1 μm GaAs buffer layer at around 600 °C [18]. It is noted that conventional III-V blanket heteroepitaxy on planar Si wafers generally requires a 4°-6° offcut angle for a prominent double stepped Si surface to prevent antiphase-domain formation. Recent studies suggested single domain Ge and III-V layers can be deposited on standard nominal Si (001) substrates through an APD annihilation mechanism [18–21]. In this study, Si (001) substrates without any specified offcut angle have been used for both templates and antiphase boundaries–free epilayers were achieved. On the two GaAs-on-(001) Si templates and another native GaAs substrate, micro-disk laser active regions were grown using molecular beam epitaxy (MBE). 1-μm GaAs buffer and a 600-nm $Al_{0.7}Ga_{0.3}As$ sacrificial layer were deposited first, followed

Optics EXPRESS

by a five-stacked InAs dot-in-a-well (DWELL) structure [22] sandwiched by 50 nm $Al_{0.4}Ga_{0.6}As$ cladding layers.

Characterization of crystal defects was carried out by TEM imaging using a JEOL2010F field-emission microscope operating at 200 keV. Taken along the [110] zone axis, the bright-field cross-sectional TEM images in Figs. 1(a) and 1(b) present the complete structures of the MDLs grown on GoVS and planar Si, respectively. We observe much reduced defects threading upwards in the GoVS template. Figures 1(c) and 1(d) show a zoomed-in view of the active region consisting of five-stacked InAs DWELLs. As opposed to the clean structure on the GoVS template, dislocation lines frequently penetrate through the active region on the planar Si template. In addition, the TEM images revealed a great difference in interface abruptness of the DWELL structures. While the interface is well defined and flat on the GoVS template, surface undulations were uncovered on the planar Si. Plan-view TEM measurements indicated a threading dislocation density of 1.4×10^8 cm^{-2} in the active region on the GoVS template, while three times the value (5.0×10^8 cm^{-2}) was observed on the planar Si. Typical plan-view TEM images on the V-groove patterned and unpatterned Si are shown in Figs. 1(e) and 1(f), respectively.

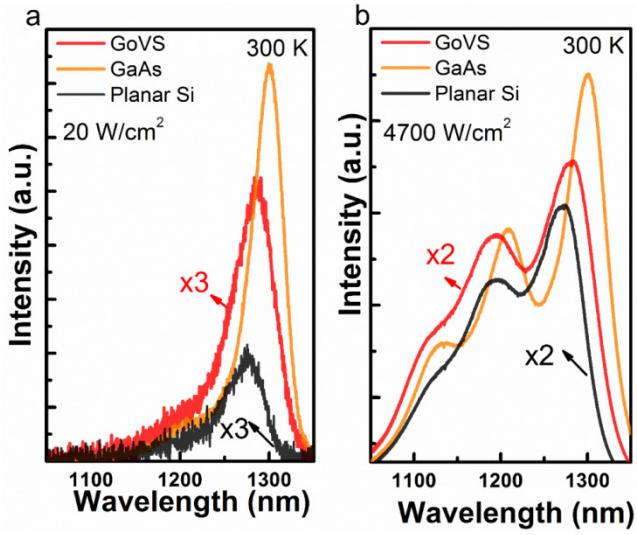

Fig. 2. Room temperature PL of the as-grown structure on GoVS template, GaAs substrate and planar Si template at pump power densities of (a) 20 W/cm^2 and (b) 4700 W/cm^2.

Figure 2 compares room temperature PL of the as-grown epitaxial structure on the three substrates. At a low pump power density of 20 W/cm^2 in Fig. 2(a), non-radiative recombination acts as the dominant quenching mechanism, precluding efficient luminescence from QDs. The difference in the luminescence closely reflects varied defect levels in the GaAs templates. Compared to the reference QDs on the GaAs substrate, the integrated PL intensity of the QDs was degraded by more than a factor of 9 on the planar Si, whereas one third degradation was observed on the GoVS template. This suggests superior optical efficiency using V-grooved Si, compared to simple planar Si. At a high pump power density of 4700 W/cm^2 in Fig. 2(b), we observe only slightly weaker luminescence on the planar Si than on the GoVS template. This is probably because at such a high pumping level, defects are mostly saturated. In Fig. 3(a), a high-resolution TEM image of an InAs quantum dot on the GoVS template is presented, showing a typical dot size of ~21 nm in diameter and ~6 nm in height.

Optics EXPRESS

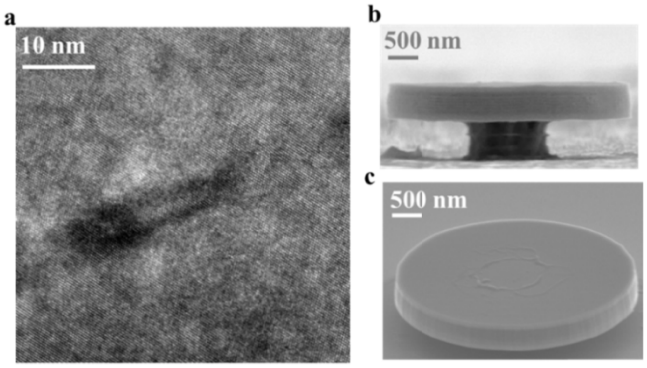

Fig. 3. (a) High-resolution TEM image revealing the typical size and shape of the quantum dots; (b) 90° tilted and (c) 70° tilted SEM image of the fabricated MDL.

Micro-disk lasers with a diameter of 4 μm were fabricated by combining colloidal lithography, dry-etching and subsequent wet-etching processes [15, 16]. The disk etching was conducted simultaneously on the three templates. Although irregularly distributed disks by colloidal lithography and process variations inevitably resulted in MDs with imperfect shapes (such as clustered together), the isolated ones exhibited sidewall roughness at a similar level on different templates, according to scanning electron microscope (SEM) observations. Typical 90°- and 70°- tilted SEM images of the fabricated devices are shown in Figs. 3(b) and 3(c), respectively. Smooth sidewalls as well as circular geometries can be clearly seen. The devices were then characterized using micro-photoluminescence (μPL) in a surface-normal pump/collection configuration. The pumping beam was from a continuous-wave (CW) diode laser at 532 nm focused to ~4 μm in diameter. For each device that is measured, careful optical alignment (including both the focus and positioning) was carried out to ensure maximum emission intensity is obtained.

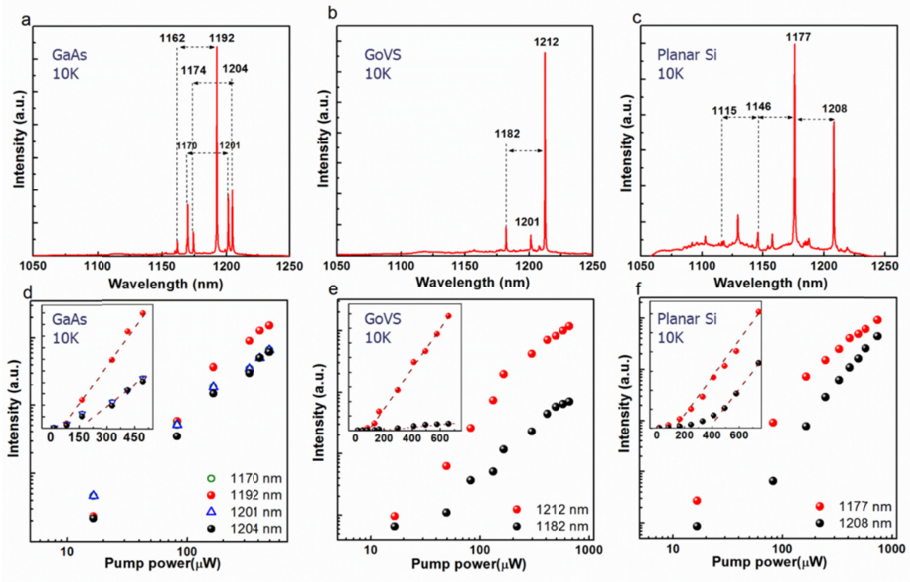

Fig. 4. Laser emission spectra at 10 K for MDLs on (a) GaAs substrate, (b) GoVS template, and (c) planar Si template; L-L curve in the log-log scale at 10 K for (d) GaAs substrate, (e) GoVS template, and (f) planar Si template. Inset: L-L curve in the linear scale, the dashed line represents a linear fit to the experimental data.

Optics EXPRESS

Low temperature lasing characteristics were measured with the samples mounted in a helium gas flow cryostat and cooled to 10 K. The representative lasing spectra at 3 times threshold are presented in Figs. 4(a)-4(c). The spectra comprise of whispering-gallery modes (WGMs) of different radial and azimuthal orders. Dotted arrows were used to connect WGMs with the same radial order. The free spectral range (FSR) was extracted to be around 30 nm. While distinct lasing peaks were observed for all three samples, the MDL on GaAs exhibited the most significant suppression of background emission, indicating the most efficient coupling of the emitter to the surrounding cavity. In contrast, the MDL on planar Si exhibited the smallest extinction ratio of ~12 dB. This is presumably attributed to the highest density of defects in the epitaxial layer compared with the other two, such that the quenching effect from non-radiative recombination is more prominent. Furthermore, the deep levels associated with the dislocations can also leach away the photogenerated carriers that are generated outside the active region. Light-in light-out (L-L) lasing curves in the log-log scale at 10 K for the three samples are presented in Figs. 4(d)-4(f). The S-shaped nonlinear characteristics clearly indicate the evolution from spontaneous emission to lasing. Thresholds were determined through a linear fit to the higher-power region of the L-L curves in linear scale, as shown in the insets of Figs. 4(d)-4(f). The thresholds of the dominant mode were determined to be ~50, 85, and 150 μW for the MDLs on the GaAs substrate, the GoVS template, and the planar Si template, respectively.

Figures 5(a)-5(c) display representative room temperature lasing emission spectra of the MDLs on the GaAs substrate, the GoVS, and the planar Si template, respectively. Note that a pronounced background emission was observed on planar Si. From the linear L-L curve shown in the insets in Figs. 5(a)-5(c), the lasing thresholds were extracted to be ~100, 135, and 265 μW for the MDLs on the GaAs substrate, the GoVS template, and the planar Si template, respectively.

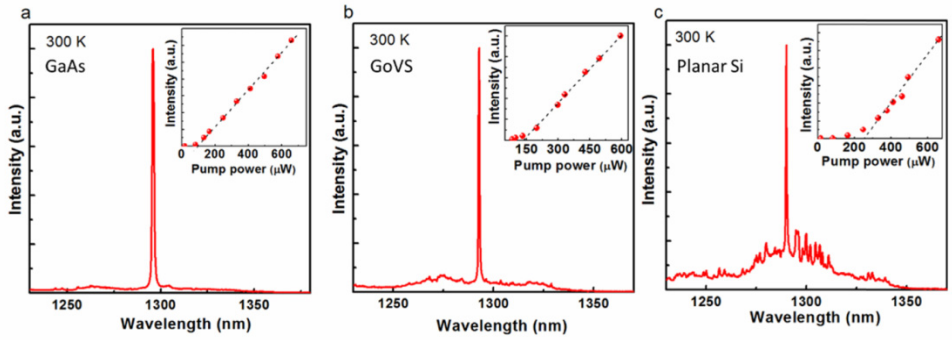

Fig. 5. Laser emission spectra at 300 K for MDLs on (a) GaAs substrate, (b) GoVS template, and (c) planar Si template. Inset: L-L curve in linear scale, the dashed line represents a linear fit to the experimental data.

Statistical analysis over some sampling of micro-disks were performed to reach a fair comparison. Histograms of the thresholds over a number of devices at 10 K and 300 K for the MDLs on the three templates are presented in Figs. 6(a)-6(f). The overall lasing thresholds of the MDLs on the GoVS template were much lower compared to those on planar Si. Notably, at 300 K, the threshold of the best working device on the GoVS template (135 μW) yielded a ~2-fold reduction compared to the best one on the planar Si template (265 μW), and was only around 1.35 times that of the best reference MDL (100 μW) on GaAs. The low-threshold laser operation under room temperature continuous-wave optical pumping presents a solid evidence of the high optical properties of the III–V crystals monolithically grown on Si. Currently, our epitaxial structure does not adopt any dislocation filtering layers. It has been reported that four

Optics EXPRESS

sets of $In_{0.18}Ga_{0.82}As$/GaAs strained-layer superlattices (SLSs) may further reduce the dislocation density in the hetero-epitaxy of GaAs on Si [12]. We therefore expect better device performance by adding effective dislocation filters in the GaAs on Si buffer, as well as by improving the uniformity of the QDs to enhance active modal gains.

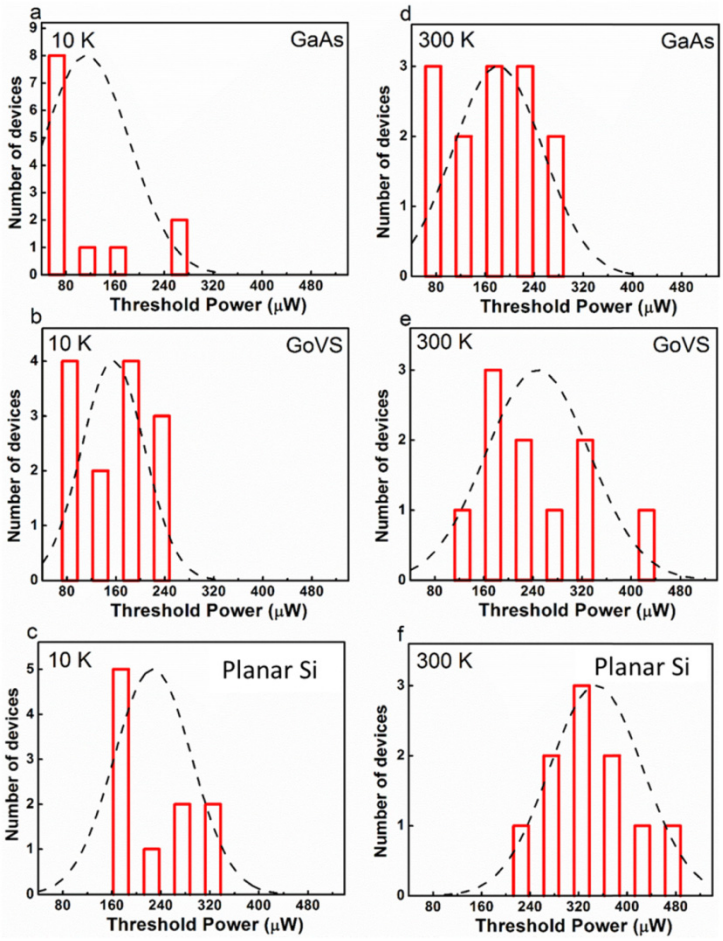

Fig. 6. Histograms of the lasing thresholds over a number of devices at 10 K for MDLs on (a) GaAs substrate, (b) GoVS template, and (c) planar Si template. Histograms of the threshold over a number of devices at 300 K for MDLs on (d) GaAs substrate, (e) GoVS template, and (f) planar Si template.

An important aspect of integrating active devices on Si is that the Si substrate is not only used as a substrate carrier but also can be used as waveguiding material because of the low optical material losses. The GoVS templates used in this work do not include any absorptive germanium buffer or other dislocation filter layers. Thus, it allows coupling from the laser active regions to Si waveguides and suggests potential opportunity to be incorporated in the well-developed silicon-on-insulator (SOI) technology in Si photonics. However, one concern for mode coupling into underlying patterned Si waveguide is that the V-grooves would add a significant amount of scattering loss. A. Liu *et al.* recently proposed one approach to achieve waveguide coupling by growing III–V cavity in selectively V-groove patterned regions on the handle wafer of a SOI substrate [11]. The optical mode is butt-coupled to a silicon rib waveguide and the optical coupling can be maximized by aligning the height of the active quantum dot region with the Si waveguide layer.

Optics EXPRESS

3. Conclusions

In conclusion, low-threshold micro-disk lasers with compact optical cavities were demonstrated on (001) Si substrates using different epitaxial schemes. A comprehensive comparison of the lasing dynamics was made in devices with the same active structures and geometries but fabricated on different GaAs-on-Si templates, from 10 K up to room temperature. Compared to GaAs on Si by conventional blanket heteroepitaxy, the GoVS template using V-groove patterned heteroepitaxy exhibited improved material quality and thereby greatly enhanced optical efficiency, as reflected by the superior lasing characteristics. The somewhat forgiving nature of QD lasers is also demonstrated by room temperature lasing of MDLs grown on simple GaAs on planar Si templates. This work therefore closes the gap between III-V lasers epitaxially grown on lattice-matched substrates and dissimilar Si substrates, illuminating a promising path towards low-threshold on-chip laser sources for high-density, high-speed data interconnections.

Funding

This work was supported the Research Grants Council of Hong Kong (Grant Nos. 614813 and 16212115) and by a DARPA MTO EPHI grant.

Acknowledgements

The authors would like to thank SUNY Poly for providing the initial nano-patterned Si substrates, Wuhan National Laboratory for Optoelectronics (WNLO) for providing the facilities to perform optical measurements, and the NFF and MCPF of HKUST for technical support. Helpful discussions with C. Zeng, Y. Zhang and Y. Geng are also acknowledged.